6-^{18}F-Fluoro-L-Dihydroxyphenylalanine Positron Emission Tomography Is Superior to ^{123}I-Metaiodobenzyl-Guanidine Scintigraphy in the Detection of Extraadrenal and Hereditary Pheochromocytomas and Paragangliomas: Correlation with Vesicular Monoamine Transporter Expression

C. Fottner, A. Helisch, M. Anlauf, H. Rossmann, T. J. Musholt, A. Kreft, S. Schadmand-Fischer, P. Bartenstein, K. J. Lackner, G. Klöppel, M. Schreckenberger, and M. M. Weber*

Context: Pheochromocytomas (PHEOs) and paragangliomas (PGLs) may be better detected by ^{18}F-fluorodihydroxyphenylalanine-positron emission tomography (FDOPA-PET) than ^{123}I-metaiodobenzyl-guanidine (123-I-MIBG) scintigraphy.

Objective: The objective of the study was to correlate functional imaging results with immunohistochemical, molecular-genetic, and biochemical findings.

Design and Setting: Thirty consecutive patients with suspected PHEO/PGL presenting at a tertiary referral centre were investigated in a prospective study.

Patients: Twenty-five patients had confirmed PHEO/PGL. Thirteen of 25 patients had a hereditary PHEO/PGL syndrome (two multiple endocrine neoplasia II, six succinate dehydrogenase complex, subunit D, two succinate dehydrogenase complex, subunit B, one von Hippel Lindau tumor suppressor protein, two Neurofibromatosis-1), and 12 of 25 were classified as sporadic. Five patients had hormonally inactive adrenal incidentalomas.

Main Outcome Measures: In all patients computed tomography scan and/or magnetic resonance imaging as well as both 123-I-MIBG scintigraphy and FDOPA-PET were performed. Resected tumors were examined by immunohistochemistry for expression of the vesicular monoamine transporter (VMAT)-1 and -2 and other markers.

Results: A total of 64 lesions were found with both functional imaging modalities. FDOPA-PET detected 62 lesions, whereas only 34 lesions were detected by 123-I-MIBG scintigraphy. This resulted in an overall sensitivity and specificity for FDOPA-PET of 98 and 100% and for MIBG of 53 and 91%, respectively. Comparable sensitivities were found for adrenal and extraadrenal abdominal lesions (94 *vs.* 97%), whereas in thoracic/cervical lesions, the sensitivity for 123-I-MIBG scintigraphy (15%) was inferior to that of FDOPA-PET imaging (100%). Immunohistochemistry demonstrated a lack of VMAT-1 expression in all MIBG-negative tumors. Clinical predictors for MIBG negativity were a predominant norepinephrine/normetanephrine secretion, an age less than 45 yr, and a hereditary cause.

Conclusion: FDOPA-PET is superior to 123-I-MIBG scintigraphy in patients with extraadrenal, predominantly noradrenaline-secreting, and hereditary types of PHEO/PGL. The lack of VMAT-1 expression predicts negativity for MIBG-scintigraphy. **(*J Clin Endocrinol Metab* 95: 2800–2810, 2010)**

ISSN Print 0021-972X ISSN Online 1945-7197
Printed in U.S.A.

doi: 10.1210/jc.2009-2352 Received November 4, 2009. Accepted March 5, 2010.
First Published Online April 6, 2010
* Author affiliations are shown at the bottom of the next page.

Abbreviations: CgA, Chromogranin A; CT, computed tomography; FDOPA, ^{18}F-fluorodihydroxyphenylalanine; ^{18}F-FDA, fluorine-18-fluorodopamine; 123-I-MIBG, ^{123}I-metaiodobenzyl-guanidine; MEN, multiple endocrine neoplasia; MRI, magnetic resonance imaging; NET, norepinephrine transporter; NF, Neurofibromatosis-1; NPV, negative predictive value; PET, positron emission tomography; PGL, paraganglioma; PHEO, pheochromocytoma; PPV, positive predictive value; SDHB, succinate dehydrogenase complex, subunit B; SDHD, succinate dehydrogenase complex, subunit D; TH, tyrosine hydroxylase; VHL, von Hippel Lindau tumor suppressor protein; VMAT, vesicular monoamine transporter.

Pheochromocytomas (PHEOs) are rare tumors arising from chromaffin cells of adrenal medullary or extraadrenal paraganglionic tissue. The World Health Organization classification of endocrine tumors defines a pheochromocytoma as an intraadrenal paraganglioma (PGL), whereas closely related tumors of extraadrenal sympathetic or parasympathetic paraganglia are classified as extraadrenal PGLs. Extraadrenal sympathetic PGLs are most frequently found in the abdomen and pelvis and to a lesser extent in the thorax, whereas parasympathetic PGLs are predominantly located in the head and neck region (1–3). In contrast to parasympathetic PGLs, which rarely synthesize significant amounts of catecholamines, PHEOs and extraadrenal sympathetic PGLs produce and secrete catecholamines and their metabolites.

Up to 25% of patients with PHEO or PGL are carriers of germline mutations of one of the four so far known genes predisposing for hereditary, usually multifocal PHEOs and PGLs like the RET-, VHL-, NF-1- or SDHx gene (4, 5). Because there are no clinical, imaging, or laboratory criteria safely predicting multiplicity and/or malignancy in these tumors, all patients with biochemically confirmed PHE/PGL should be screened for metastatic disease or multiple tumors. The localization of PHEO/PGL is generally performed by computed tomography (CT) or magnetic resonance imaging (MRI), which show a good sensitivity for detecting these tumors but lack the specificity required to unequivocally identify a mass as a PHEO or PGL. Although a generally accepted and cost-effective approach for the diagnostic localization of PHEO/PGL has yet to be established, there is clear agreement that functional imaging is useful to detect multifocal or metastatic disease (6).

Up to now, 123-I-metaiodobenzylguanidine (MIBG) scintigraphy is the standard functional imaging procedure to detect multifocal PHEOs or PGLs (7). MIBG is a guanethidine analog resembling norepinephrine. It is taken up by sympathomedullary tissue via the norepinephrine transporter (NET) and deposited in storage granules, which is mediated by the vesicular monoamine transporters (VMAT) types 1 and 2 (8). Thus, the expression of vesicular monoamine transporters is assumed to be a prerequisite for functional imaging. Recently the expression of both VMATs has been demonstrated in normal adrenal medulla and pheochromocytomas (8, 9).

123-I-MIBG scintigraphy has been widely used for more than 25 yr and has a reported sensitivity of approximately 83–100% and a specificity of 85–100%. However, 123-I-MIBG scintigraphy has several major disadvantages. It has a low spatial resolution, long duration of the procedure (48 h), necessity to block thyroid accumulation, interference with medications, and a significant tracer-uptake in the normal adrenal medulla (8). Recently published data indicate that its sensitivity is far less than previously reported, especially for the detection of extraadrenal or metastatic disease, in which the sensitivities do not exceed 65%. Additionally, with the distinction of sporadic and hereditary PHEO syndromes, 123-I-MIBG scintigraphy was found to have a highly variable positivity in a subset of pheochromocytoma patients (8, 10, 11). Therefore, new radiotracers, in particular for positron emission tomography (PET), have been developed. Recently the ^{18}F-labeled catecholamine fluorine-18-fluorodopamine (^{18}F-FDA) and the catecholamine precursor fluorine-18-dihydroxyphenylalanine (^{18}F-FDOPA) have been used as PET tracers for imaging of neuroendocrine tumors, especially PHEOs and PGLs (12–15).

These compounds have been developed based on the capability of neuroendocrine cells for specific uptake and subsequent decarboxylation of amino acids. DOPA can be decarboxylated to dopamine by the enzyme L-amino acid decarboxylase, which is strongly expressed in neuroendocrine cells and shows high affinity to ^{18}F-FDOPA. After decarboxylation of ^{18}F-FDOPA to ^{18}F-FDA, it is transported to and stored in intracellular vesicles in which it can be visualized for imaging purposes (16). The advantages of this technique are a quick performance within 2 h, a superior spatial resolution, no interference with medications, and in general no relevant physiological tracer uptake in normal adrenal medulla (at least for ^{18}F-FDOPA). Several smaller studies showed an excellent sensitivity equivalent or superior to 123-I-MIBG scintigraphy in patients with known or suspected benign and malignant PHEOs and PGLs (17–20). It has been suggested that ^{18}F-FDA PET or ^{18}F-FDOPA-PET might be a superior functional imaging modality in patients with adrenal PHEOs associated with the von Hippel-Lindau syndrome and patients with extraadrenal PGLs associated with mutations in the SDHD gene (21, 22).

In a recently published larger prospective study in 48 patients with proven catecholamine excess, FDOPA-PET was superior to both 123-I-MIBG scintigraphy and CT/MRI for the localization of catecholamine-producing tumors (23). However, in this study almost exclusively adrenal PHEOs and no relevant number of extraadrenal tumors have been investigated. Additional shortcomings of all the aforementioned studies are the lack of a histological verification of the investigated lesions. Furthermore, nothing is known so far

I. Medical Clinic (C.F., M.M.W.), Departments of Nuclear Medicine (A.H., M.S.) and Radiology (S.S.-F.), Institute for Clinical Chemistry (H.R., K.J.L.), Section of Endocrine Surgery (T.J.M.), and Institute of Pathology (A.K.), University of Mainz, 55131 Mainz, Germany; Institute of Pathology (M.A.), University of Duesseldorf, 40225 Duesseldorf, Germany; Department of Nuclear Medicine (P.B.), Ludwig-Maximilians University, 80539 Munich, Germany; and Institute of Pathology (G.K.), Technical University, 80802 Munich, Germany

about the molecular basis of the different sensitivities of FDOPA-PET and 123-I-MIBG scintigraphy found in patients with sporadic and hereditary PHEOs or PGLs.

The aim of this prospective study was therefore to compare the sensitivity and specificity of FDOPA-PET with that of 123-I-MIBG scintigraphy in a series of patients with sporadic and familial PHEOs/PGLs of different locations and the functional imaging results with clinical, immunohistochemical, molecular genetic, and laboratory parameters.

Subjects and Methods

Subjects

For biochemical evaluation, 24-h urinary fracA total of 30 consecutive patients (16 female, 14 male) with biochemical catecholamine excess (n = 24), proven hereditary PHEO/PGL syndrome (n = 1), or an adrenal incidentaloma greater than 5 cm (n = 5) who presented at the outpatient clinic of the university medical center Mainz between January 2005 and June 2007 were included in this study. Twenty-four patients had increased catecholamine secretion (elevated 24 h urinary free meta-/normetanephrines and/or 24 h urinary epinephrine, norepinephrine, and dopamine levels in at least one of three consecutive 24 h urine samples), and one patient was previously diagnosed having a mutation in the SDHD gene after molecular-genetic counseling of an affected family member with consecutive mutation screening (without biochemical catecholamine excess). Twenty-five patients (15 male, 10 female) had histologically confirmed PHEO/PGL. Thirteen patients had hereditary PHEO/PGL syndromes [two multiple endocrine neoplasia (MEN) II, six succinate dehydrogenase complex, subunit D (SDHD), two succinate dehydrogenase complex, subunit B (SDHB), one von Hippel Lindau tumor suppressor protein (VHL), two Neurofibromatosis-1 (NF)-1, mean age 39.5 yr]; the remaining 12 (mean age 44.1 yr) were classified as sporadic. Five patients with biochemically excluded diagnosis of pheochromocytoma had an adrenal incidentaloma greater than 5 cm and served as controls. Histological analysis revealed adrenocortical adenomas in all cases.

After biochemical evaluation, all patients were further investigated using both 123-I-MIBG scintigraphy and FDOPA-PET, respectively. In all patients with a detected lesion by functional imaging (n = 26), the respective body region was additionally examined with MRI or CT scan, and images were correlated with functional imaging results. In case of a proven catecholamine excess and/or a positive functional imaging procedure (n = 26) or in case of an adrenal incidentaloma with a size greater than 5 cm (n = 5), the patients underwent surgical removal of the tumor. All surgically removed tumors were examined for expression of the VMAT-1 and -2, tyrosine hydroxylase (TH), chromogranin A, synaptophysin, and KI-67. Imaging results were correlated with immunohistochemical, molecular-genetic, and biochemical findings (see Table 1). The study was performed according to the guidelines of the local ethical committee and all patients or their legal representatives gave written informed consent.

123-I-MIBG scintigraphy and FDOPA-PET imaging

Medication known to interfere with ^{123}I-MIBG scintigraphy was withdrawn and patients received 250 MBq ^{123}I-MIBG after thyroid blocking with perchlorate (300 mg twice a day). For γ-imaging a triple-head camera (IRIX; Philips, Cleveland, OH) was used, and anterior and posterior body scans were performed 4 and 24 h after injection with a 256- $\times$ 1024-pixel matrix; for comparison with CT scans additional single photon emission computed tomography data were acquired at the same time points: 120 views per three, 45 sec/view, 128 $\times$ 128 matrix, iterative reconstruction. PET imaging was done with the ECAT EXACT 922 scanner (Siemens/CTI, Knoxville, TN) in three-dimensional mode starting 60–80 min after the injection of 238 MBq (range 160–253 MBq) ^{18}F-DOPA with attenuation correction: six to eight bed positions of 6 min emission and 2-min transmission scans. Images were reconstructed by ordered subset expectation maximization algorithm with two iterations and eight subsets on a Sun workstation using ECAT standard software.

For both imaging modalities, adrenal uptake and extraadrenal nonphysiological lesions were compared with physiological liver uptake. A lesion was considered to be positive if its tracer uptake exceeded that of the liver. Imaging interpretation was performed by one experienced nuclear medicine physician, blinded for any other clinical or biochemical information. Interpretation of 123-I-MIBG scintigraphy and FDOPA-PET scans was performed during separate reading sessions.

CT/MRI

All lesions found with functional imaging underwent CT or MRI imaging before surgical removal to determine the appropriate surgical procedure. CT or MRI was chosen depending on the body region to be examined and individual patient requirements or based on the preference of the treating physician and the surgeon. CT examinations were performed using a multislice scanner, both before and after administration of iv contrast agent. MRI examination was performed on a 1.0 Tesla scanner using T1- and T2-weighted sequences, including series after administration of an iv contrast agent. Reconstructed slice thickness varied between 2 and 10 mm.

Biochemical markers

For biochemical evaluation, 24-h urinary fractionated metanephrines/normetanephrines were determined. Urinary fractionated metanephrines (reference range 20–345 μg/d) and normetanephrines (reference range 30–440 μg/d) and serum chromogranin A (CgA; reference range <98 ng/ml) were analyzed by RIAs [MetCombi RIA (urine), IBL International GmbH, Hamburg, Germany; CGA-RIA CT, Cis Bio International, Sorgues, France].

Immunohistochemistry

Immunohistochemical analysis was performed as described previously (24). Briefly, serial tissue sections from formalin-fixed paraffin specimens were stained with hematoxylin and eosin and for immunohistochemical analysis with the following antibodies: CgA LK 2H10 (Boehringer, Mannheim, Germany) 1:200, mouse monoclonal; Synaptophysin M0010 (Dako, Hamburg, Germany), 1:50; rabbit polyclonal VMAT1 [PNAS 93:5166–5171 (29)], 1:3000; rabbit polyclonal VMAT2, 0182 [PNAS 93:5166–5171 (29)]; 1:3000 rabbit polyclonal TH, 2/40/15 (Boehringer) 1:80, mouse monoclonal. Deparaffinized tissue sections were rehydrated and subjected to heat-induced epitope retrieval procedures as described previously. After blocking with nonimmune serum, the sections were incubated with the primary

TABLE 1. Clinical and immunohistochemical characteristics of 25 patients with histologically proven PHEOs and PGLs

							Clinical evaluation					Histological evaluation					
Patient	Age (yr)	Gender	Genetics	Tumor type	Size/lesions (cm/n)	Metastasis	Serum CgA (× ULN)	Metanephrine (× ULN)	Normetanephrin (× ULN)	MIBG	FDOPA-PET	VMAT-1	VMAT-2	TH	CgA	Syn	KI-67
1	57	♀	Sporadic	PHEO	2.0, 2	+	1936 (19.76)	1200 (3.48)	1561 (3.55)	Pos.	Pos.	6+	6+	6+	6+	6+	10%
2	48	♂	Sporadic	PHEO	5.6	−	1061 (10.83)	1200 (3.48)	4200 (9.55)	Pos.	Pos.	5+	6+	6+	6+	6+	2%
3	39	♂	Sporadic	PHEO	6.0	−	277 (2.83)	3000 (8.70)	256 (9.67)	Pos.	Pos.	6+	6+	6+	6+	6+	2%
4	26	♂	Sporadic	PHEO	5.3	−	120 (1.22)	12968 (37.59)	10560 (24.0)	Pos.	Pos.	6+	6+	6+	6+	6+	2%
5	66	♂	Sporadic	PHEO	2.8	−	246 (2.51)	103 (0.30)	589 (1.34)	Pos.	Pos.	6+	6+	6+	6+	6+	2%
6	41	♂	Sporadic	PHEO	4.0	−	95 (0.97)	580 (1.68)	6875 (15.63)	Neg.	Pos.	1+	6+	6+	6+	6+	2%
7	41	♀	Sporadic	PHEO	8.0, 7	+	6997 (71.40)	3930 (11.39)	9705 (22.06)	Pos.	Pos.	6+	6+	n.a.	n.a.	6+	n.a.
8	52	♀	Sporadic	PHEO	4.0	−	1410 (14.39)	177 (0.51)	2618 (5.95)	Neg.	Pos.	1+	6+	6+	1+	6+	5%
9	28	♀	Sporadic	PHEO	7.0	−	1798 (18.35)	2200 (6.38)	3449 (7.84)	Pos.	Pos.	5+	6+	6+	6+	6+	2%
10	48	♀	Sporadic	PHEO	4.0	−	141 (1.44)	1801 (5.2)	1248 (2.84)	Pos.	Pos.	6+	6+	6+	6+	6+	<2%
11	36	♀	Sporadic	PHEO	5.0	−	214 (2.18)	1092 (3.17)	1560 (3.55)	Pos.	Pos.	6+	6+	6+	6+	6+	2%
12	47	♀	Sporadic	PHEO	6.0, 6	+	381 (3.89)	1111 (3.22)	1845 (4.19)	Pos.	Pos.	6+	6+	6+	6+	6+	10%
13	66	♀	MEN IIa	PHEO	3.0	−	198 (2.02)	1486 (4.31)	1250 (2.84)	Pos.	Pos.	6+	6+	6+	6+	6+	2%
14	38	♂	MEN IIa	PHEO	4.0	−	154 (1.57)	512 (1.48)	888 (2.02)	Pos.	Pos.	6+	6+	6+	6+	6+	1%
15	28	♀	VHL	Bilateral PHEO	7.0, 2	−	169 (1.72)	53 (0.15)	1584 (3.60)	Pos.	Pos.	6+	6+	6+	6+	6+	2%
16	57	♀	NF-1	PHEO	3.5, 2	+	158 (1.61)	571 (1.66)	855 (1.94)	Pos.	Pos.	6+	6+	6+	6+	6+	5%
17	52	♀	NF-1	PHEO	2.0	−	132 (1.35)	552 (1.60)	1619 (3.68)	Pos.	Pos.	6+	6+	6+	6+	6+	2%
18	45	♂	SDHD	Bilateral PHEO	2.5, 2	−	130 (1.33)	94 (0.27)	1511 (3.43)	Pos.	Pos.	6+	6+	6+	5+	6+	2%
19	46	♀	SDHD	PGL (thoracic/cervical)	3.0, 4	−	48 (0.49)	441 (1.28)	483 (1.10)	Neg.	Pos.	1+	6+	0	1+	6+	2%
20	29	♀	SDHD	PGL (thoracic/cervical)	2.0, 6	−	35 (0.36)	116 (0.34)	192 (0.44)	Neg.	Pos.	1+	6+	0	3+	6+	4%
21	43	♀	SDHD	PGL (thoracic/cervical)	4.0, 4	+	70 (0.71)	144 (0.42)	590 (1.34)	Neg.	Pos.	1+	6+	0	1+	6+	2%
22	28	♂	SDHD	PHEO + PGL (extraadr. abd.)	3.4, 5	−	208 (2.12)	398 (1.15)	4832 (10.98)	Pos.	Neg.	6+	6+	6+	6+	6+	<2%
23	14	♀	SDHD	PGL (extraadr. abd.)	3.0, 4	−	213 (2.17)	326 (0.94)	1114 (2.53)	Pos.	Pos.	6+	6+	6+	6+	6+	2%
24	30	♂	SDHB	PGL (extraadr. abd.)	2.3, 4	−	547 (5.58)	299 (0.87)	4451 (10.12)	Pos.	Pos.	6+	6+	6+	6+	6+	1%
25	38	♂	SDHB	PGL (extraadr. abd.)	3.4, 4	−	216 (2.20)	398 (1.15)	4832 (10.98)	Pos.	Pos.	6+	6+	6+	6+	6+	2%

Immunohistochemical evaluation of marker-expression: −, 0%; +, less than 10%; 2+, 10 to greater than 20%; 3+, 20 to less than 40%; 4+, 40 to less than 60%; 5+, 60 to less than 80%; 6+, 80–100%. Syn, Synaptophysin; Ki-67, MIB1 proliferation index; ULN, upper limit of normal; Pos, positive; Neg, negative; n.a., not available; extraadr. abd., extraadrenal abdominal.

antibody (45 min), followed by species-specific biotinylated secondary antibodies (45 min; Dianova, Hamburg, Germany). After being washed, the slides were incubated with the ABC reagents for 30 min (Vectastain Elite ABC kit; Boehringer, Ingelheim, Germany). The immunoreaction was visualized with 3′3-diaminobenzidine (Sigma, Deisenhofen, Germany) and counterstained with hematoxylin. Sections were analyzed and photographed with an Axioskop 50 microscope (Zeiss, Oberkochen, Germany). The number of VMAT-1 and VMAT-2-immunoreactive cells in tumors was estimated semiquantitatively and scored on a scale from − (absent); +, less than 10%; 2+, 10 to greater than 20%; 3+, 20 to less than 40%; 4+, 40 to less than 60%; 5+, 60 to less than 80%; 6+, 80–100%. As positive controls normal tissue of human adrenal glands has been used.

Data and statistical analysis

Arithmetic means and SDs were calculated using SPSS Software, package version 14.0 (SPSS Inc., Chicago, IL). Data were analyzed using f test for testing the variance of the probability distribution and Student's *t* test for unpaired samples. Statistical significance was defined as $P < 0.05$ unless otherwise mentioned. The following computing formulas were used for evaluation of sensitivities and specificities [true negative (TN), true positive (TP), false positive (FN), false negative (FN)]: sensitivity [TP/(TP + FN)], specificity [TN/(TN + FP)], positive predictive value (PPV) [TP/(TP + FP)], negative predictive value (NPV) [TN/(TN + FN)], accuracy [(TP + TN)/(TP + TN + FN + FP)], rate of FN [FN/(FN + TP)], and rate of FP [FP/(FP + TN)]. Analysis was performed at the level of individual lesions to calculate lesion-based sensitivities. As reference standard for the presence of tumor lesions, a composite reference standard was used as previously described by Koopmans *et al.* (25). This included all available histological and follow-up findings as well as morphological imaging data because histological evaluation of every lesion was not feasible due to five patients with metastatic PHEO/PGL. However, in all patients included in this study, at least one tumor sample was available for histological evaluation. In most patients with hereditary PHEO/PGL syndromes or metastatic PHEO, multiple lesions (up to five) were available for histological evaluation. To prove the diagnosis of a PHEO/PGL and for correlation with functional imaging studies, only the histological verified lesions were included for the calculation of the lesion-based sensitivities and specificities and to qualify lesions as true-positive or -negative.

Results

Functional imaging (MIBG scintigraphy and FDOPA-PET)

In 26 of 30 patients, a total number of 64 lesions could be found with both functional imaging modalities. FDOPA-PET was positive in all patients but one with two extraadrenal abdominal paragangliomas with a diameter of 10 mm, whereas in contrast, five patients had negative 123-I-MIBG scintigraphy. All adrenal and 75% of extraadrenal abdominal lesions could be visualized by both FDOPA-PET and 123-I-MIBG scintigraphy. In contrast, only one of 19 extraadrenal thoracic and head and neck paragangliomas were positive on 123-I-MIBG scintigraphy, whereas all of them could be easily detected with FDOPA-PET. This resulted in an overall sensitivity and specificity for FDOPA-PET of 98 and 100% and of 53 and 91% for 123-I-MIBG scintigraphy, respectively (Table 2). When sensitivities and specificities were stratified by tumor localization, comparable results for both imaging modalities were found for adrenal and extraadrenal abdominal lesions (123-I-MIBG scintigraphy, 97 and 91%; FDOPA-PET, 94 and 100%). In extraadrenal thoracic and cervical lesions, however, the sensitivity for 123-I-MIBG scintigraphy (15%) was significantly inferior to that found for FDOPA-PET imaging (100%), whereas both functional imaging procedures showed an equal high specificity (100%).

Anatomical imaging

In this study, morphological imaging with either CT or MRI was used after functional imaging mainly for preoperative staging of the patients and determination of adequate surgical procedure. Even though it was not the aim of the study to compare the diagnostic utility of functional imaging *vs.* morphological imaging using CT/MRI, FDOPA-PET not only detected significantly more lesions (n = 64) than 123-I-MIBG scintigraphy (n = 34) but also identified significantly more lesions than CT or MRI. With

TABLE 2. Calculated sensitivities and specificities (percent) of functional imaging of PHEOs and PGLs with 123-I-MIBG scintigraphy and FDOPA-PET: correlation with tumor localization

	MIBG All	FDOPA-PET All	MIBG Adrenal/extraadrenal abdominal	FDOPA-PET Adrenal/extraadrenal abdominal	MIBG Extraadrenal cervical/thoracic	FDOPA-PET Extraadrenal cervical/thoracic
Sensitivity	53	98	97	94	15	100
Specificity	91	100	91	100	100	100
PPV	97	100	97	100	100	100
NPV	25	92	91	85	28	100
Accuracy	59	99	95	95	36	100
Rate of FN	47	2	3	6	85	0
Rate of FP	9	0	9	0	0	0

FN, False negative; FP, false positive.

CT/MRI, only 35 lesions were detected and especially small extraadrenal abdominal and thoracic paragangliomas failed the detection with morphological imaging studies.

Immunohistochemistry

On histological examination of the 25 operated patients with biochemically proven PHEO/PGL, all lesions found with 123-I-MIBG scintigraphy or FDOPA-PET imaging were shown to be PHEOs or PGLs, with metastasis in five cases. One of the additionally evaluated patients with an adrenal incidentaloma and borderline elevation of urinary catecholamines had a positive 123-I-MIBG scintigraphy but proved to be a cortical adenoma on histological examination. Immunohistochemically, all tumors were strongly positive for synaptophysin, whereas a positive CgA immunostaining was found in only 80% of the investigated tumors. The CgA-negative tumors were exclusively parasympathetic cervical or thoracic PGLs that failed to show an expression of the TH on immunohistochemical analysis. Interestingly, in all patients with CgA-negative tumors, normal CgA serum levels were found, even in patients with a high tumor burden due to metastatic disease. Evaluation of VMAT-1 and -2 expression in the tumors showed a strong expression of VMAT-2 in all investigated PHEOs/PGLs (Fig. 1). In contrast, VMAT-1 immunostaining was very weak (<10%) or

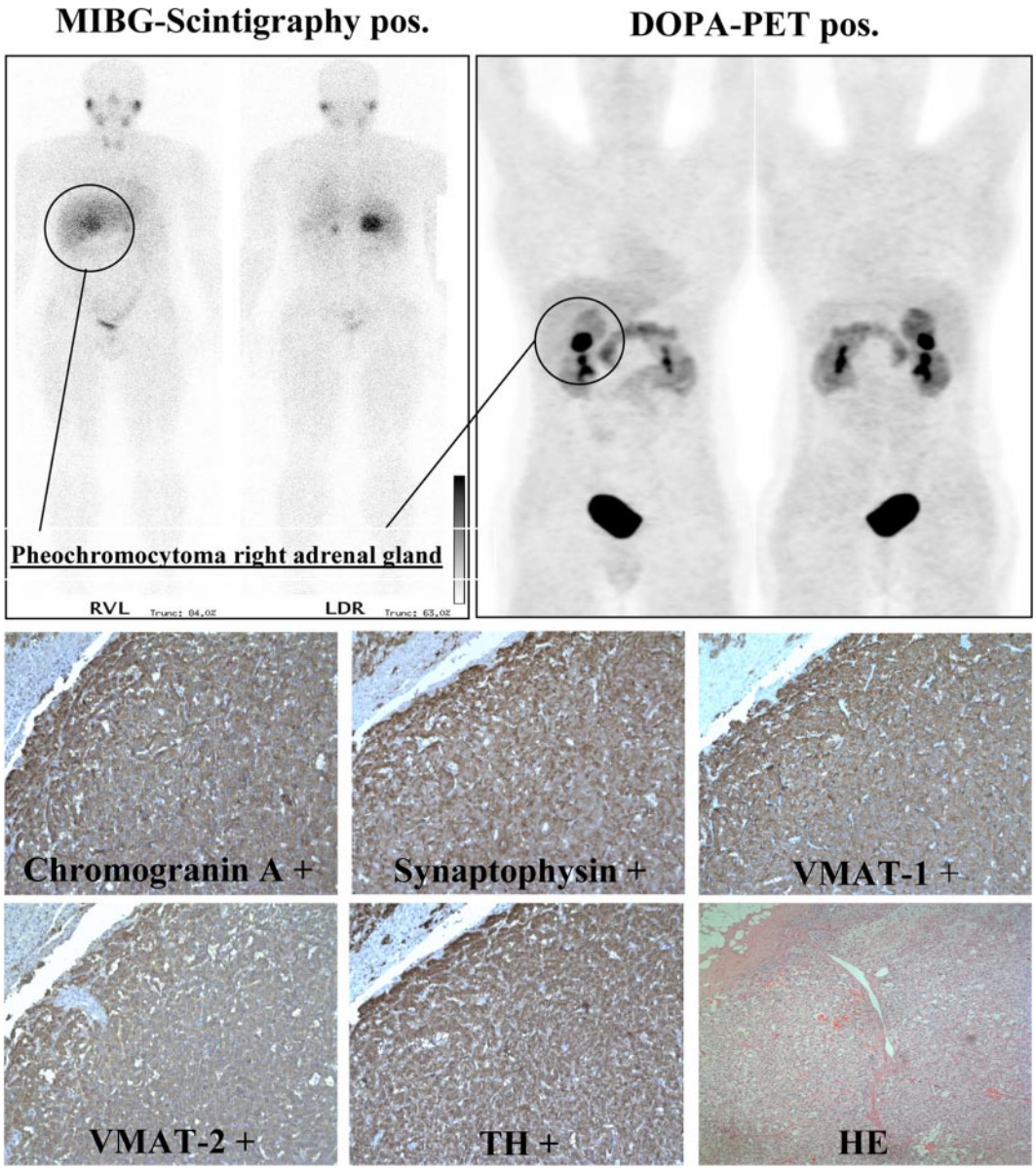

FIG. 1. Sporadic VMAT-1-positive adrenal PHEO. Functional imaging of a patient with nonsyndromic adrenal PHEO. Both 123-I-MIBG scintigraphy and FDOPA-PET are able to detect the right-sided PHEO. The resected tumor showed the immunohistochemical features of adrenal PHEO with strong expression of CgA and synaptophysin. In correlation with significantly elevated urinary free metanephrine and normetanephrine levels, the tumor expressed TH and both VMATs (VMAT-1/2).

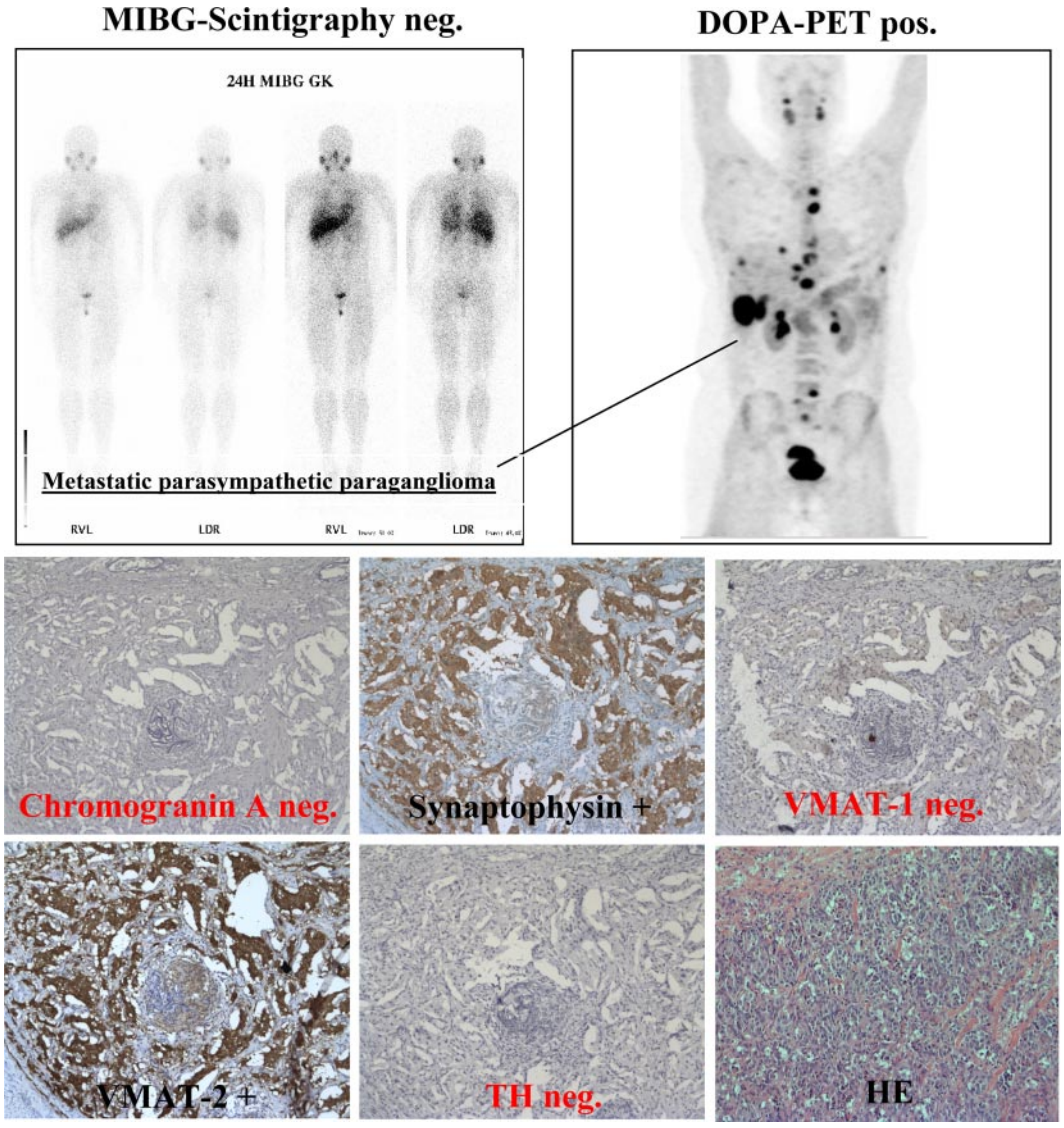

FIG. 2. VMAT-1-negative parasympathetic PGL. Functional imaging was of a patient with familial PGL syndrome type 3 and a metastatic cervical PGL with multiple lesions in the bone, liver, lung, and lymph nodes. None of the four resected lesions (two cervical head and neck PGLs and biopsies from the liver and the bone) were detected with 123-I-MIBG scintigraphy, whereas FDOPA-PET recognized even small metastatic lesions with excellent spatial resolution. Immunohistochemically the tumor specimens were negative for CgA but strongly positive for synaptophysin. In accordance with the negative catecholamine excretion, the tumor did not express TH and was therefore classified as parasympathetic PGL. Because it was found to be characteristic for MIBG-negative PGLs, no VMAT-1 was expressed.

absent in all MIBG-negative tumors (Figs. 2 and 3). Most of the VMAT-1-negative tumors showed extraadrenal localization and were parasympathetic PGLs (Fig. 2) with the exception of two large sporadic adrenal PHEOs that also had a negative 123-I-MIBG scintigraphy and did not stain for VMAT-1 (Fig. 3). Only two sympathetic extraadrenal abdominal PGLs were not detected with FDOPA-PET imaging but showed a strong signal with 123-I-MIBG scintigraphy (Fig. 4). These tumors expressed both VMAT-1 and -2 but were small tumors with a diameter of 10 mm.

Molecular genetics and biochemical markers

Because all extraadrenal PHEOs/PGLs (except two patients with sporadic but metastasized PHEO) were found can presented with a predominant norepinephin patients with hereditary pheochromocytoma syndromes, functional imaging with FDOPA-PET had a significantly higher sensitivity (96%) than 123-I-MIBG scintigraphy (40%) in patients with hereditary PHEO syndromes (Table 3). Three of five MIBG-negative patients had extraadrenal PGLs as part of a familial PGL syndrome with proven mutations in the SDHD gene. All of them presented with multifocal extraadrenal cervical and thoracic PGLs. One patient had proven metastatic disease with multiple bone, liver, lung, and lymph node metastases. The remaining two MIBG-negative patients had sporadic adrenal PHEOs. All patients who had a negative MIBG scan presented with a predominant norepinephrine and normeta-

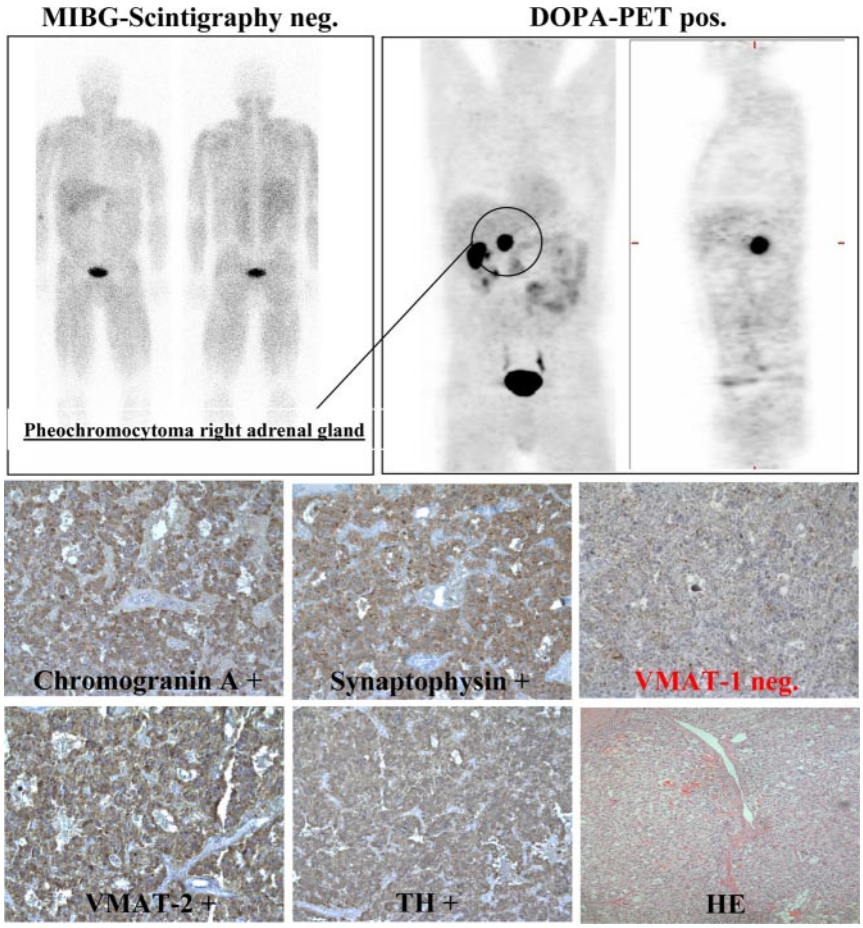

FIG. 3. Sporadic VMAT-1-negative adrenal PHEO. Functional imaging was of a patient with nonsyndromic adrenal PHEO. In contrast to FDOPA-PET imaging, the right-sided PHEO was not detected by 123-I-MIBG scintigraphy. The tumor specimen showed classical immunohistochemical features of an adrenal PHEO with strong expression of CgA and synaptophysin. In correlation with the significantly elevated urinary free metanephrines and normetanephrines, the tumor expressed TH. In contrast to MIBG-positive adrenal PHEO, this MIBG-negative PHEO expressed only VMAT-2.

nephrine secretion on biochemical evaluation. In these patients the normetanephrine levels were on average 4.89-fold above the upper limit of normal, whereas the metanephrine levels did show no relevant elevation (on average 1.17-fold above the upper limit of normal). Apart from its better sensitivity, another major advantage of FDOPA-PET imaging was its superior spatial resolution allowing the detection of small and metastatic lesions and even the identification of two synchronous intraadrenal PHEOs in a MEN II patient.

Discussion

Previous studies have indicated that ^{18}F-FDOPA-PET may be superior to 123-I-MIBG scintigraphy as a functional imaging technique in patients with PHEOs or PGLs (15, 16). However, so far, nothing is known about the molecular mechanisms explaining these differences. This study is the first to demonstrate that the differential expression of VMATs is closely correlated with the two functional imaging modalities. For a positive functional imaging by 123-I-MIBG scintigraphy, the expression of VMAT-1 was found to be essential because all tumors negative for VMAT-1 on immunohistochemical analysis remained undetected with 123-I-MIBG scintigraphy. In contrast, for visualization of PHEOs/PGLs with FDOPA-PET, the expression of VMAT-2 alone was sufficient because even in the absence of VMAT-1, all MIBG-negative tumors could easily be detected by FDOPA-PET imaging.

VMATs translocate monoamines from the cytosol into the secretory vesicles of monoaminergic neurons and neuroendocrine cells along an ATPase-generated proton gradient. In mammals, two closely related isoforms of the monoamine transporters termed VMAT-1 and VMAT-2 were identified (26, 27). VMAT-1 and VMAT-2 differ in their tissue distribution. VMAT-1 is usually strongly expressed in adrenal chromaffin cells. However, some adrenal chromaffin cells also express VMAT-2, but the amount of VMAT-2 relative to VMAT-1 appears much lower (28, 29). In contrast, sympathetic ganglion cells and parasympathetic paraganglia express predominantly VMAT-2 (30). This has recently been demonstrated in a large series of neuroendocrine tumors, in which all investigated PHEOs (six of six) and PGLs (12 of 12) did show a strong expression of VMAT-2 (9).

These physiological data are in good accordance with our findings, showing that all parasympathetic PGLs of the head and neck and additionally one PGL of the sympathetic trunk were VMAT-1 negative and failed to be detected by 123-I-MIBG scintigraphy. The majority of the adrenal PHEOs, on the contrary, were VMAT-1 positive and thus easily detectable by 123-I-MIBG scintigraphy, resulting in similar overall sensitivities for both functional imaging modalities. Only two of 19 PHEOs proved to be VMAT-1 negative, and these tumors consequently were also missed by 123-I-MIBG scintigraphy. These data for the first time provide a molecular explanation for the different sensitivities found for both imaging techniques because VMAT-1 expression was necessary for functional imaging of PHEO/PGL with 123-I MIBG scintigraphy.

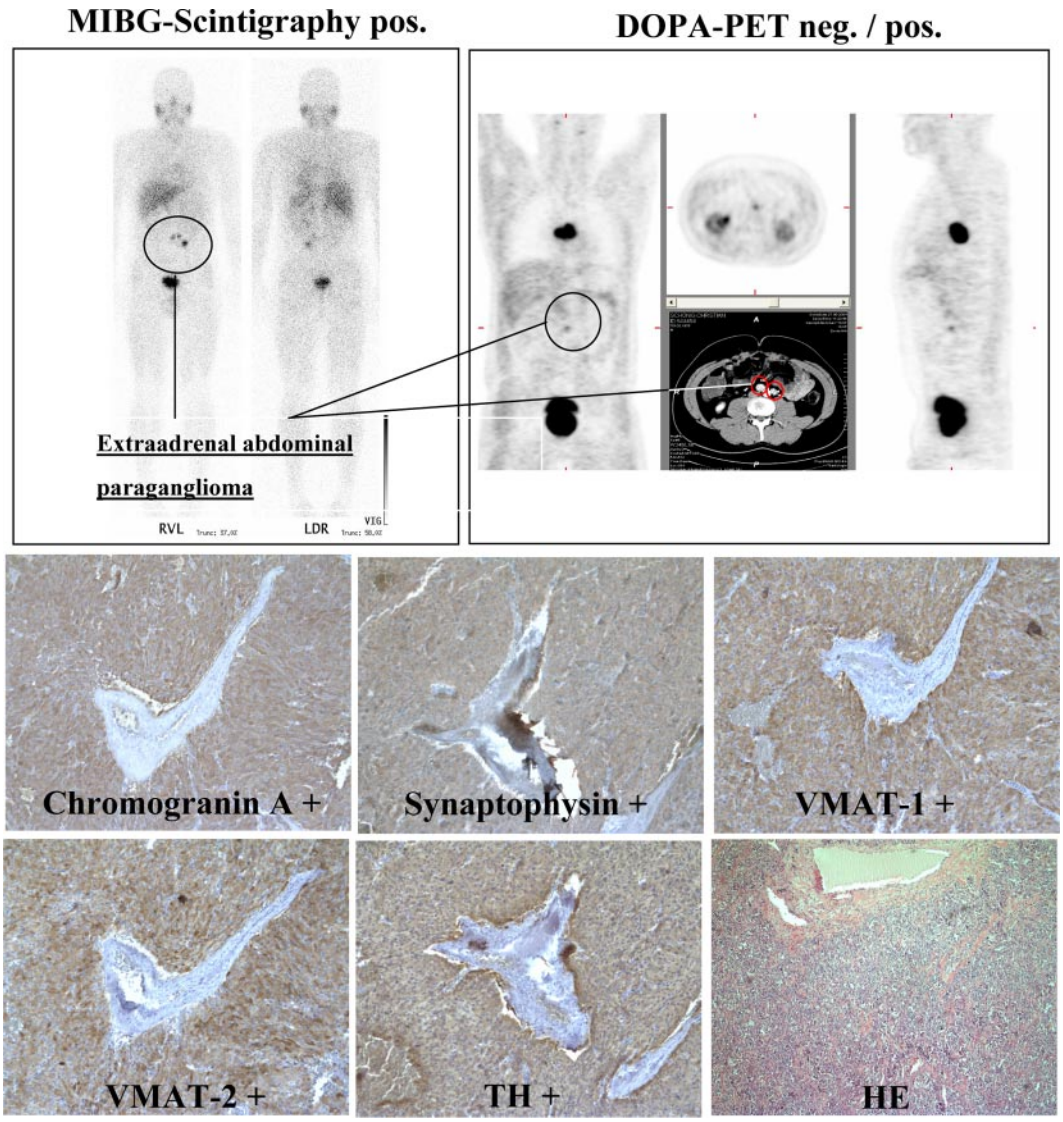

FIG. 4. Visualization of VMAT-1-positive sympathetic PGL. Functional imaging of a patient with familial PGL syndrome type 3 and multiple extraadrenal abdominal PGLs. In contrast to 123-I-MIBG scintigraphy, which detected all three paraaortal PGLs, FDOPA-PET detected only one of three PGLs. Immunohistochemically the tumor specimen showed strong expression of CgA and synaptophysin. In correlation with the significantly elevated urinary free normetanephrine levels, the tumor expressed TH and was therefore classified as sympathetic PGL. Both VMATs (VMAT-1/2) were expressed with no significant difference.

However, MIBG is a guanethidine analog resembling norepinephrine. Before its deposition in storage granules via VMATs, it is taken up by sympathomedullary tissue via the NET. Recent data show differences in NET expression in pheochromocytomas of VHL and MEN II patients (31); thus, a low or absent NET expression in PHEOs could be at least another theoretical reason for MIBG negativity.

TABLE 3. Calculated sensitivities and specificities (percent) of functional imaging of PHEOs and PGLs with 123-I-MIBG scintigraphy and FDOPA-PET: molecular genetic and biochemical characteristics

	MIBG Sporadic	FDOPA-PET Sporadic	MIBG Hereditary	FDOPA-PET Hereditary	MIBG M/NM >1.5	FDOPA-PET M/NM >1.5
Sensitivity	94	100	40	96	29	96
Specificity	91	100	91	100	100	100
PPV	94	100	95	100	100	10
NPV	91	100	26	85	24	85
Accuracy	93	100	49	97	42	97
Rate of FN	6	0	60	4	71	4
Rate of FP	9	0	9	0	0.00	0

M, Metanephrine; NM, normetanephrine.

In our study a predominant norepinephrine/normetanephrine secretion was found in PHEOs/PGLs that were negative on 123-I-MIBG scintigraphy. Thus, a preferential norepinephrine/normetanephrine secretion in conjunction with an absent or low epinephrine/metanephrine production was a strong predictor for a negative MIBG scan. This was not only true for extraadrenal PHEOs and PGLs which are known to predominantly secrete norepinephrine, but also applied for the two MIBG-negative adrenal PHEOs. This is supported by previous studies that demonstrated a significantly lower VMAT-1 expression in adrenergic *vs.* noradrenergic PHEOs on both the protein and mRNA level (31).

Even though FDOPA-PET was clearly superior in detecting PHEOs/PGLs than 123-I-MIBG scintigraphy and morphological imaging with CT/MRI, which is in good accordance with previously published data (24), overall sensitivity did not reach 100%. In our study two sympathetic extraadrenal PGLs remained undetected with FDOPA-PET imaging but have been identified with 123-I-MIBG scintigraphy. These small tumors had a diameter of 10 mm. It is unlikely that the size of these tumors was below the detection limit of this method. The spatial resolution of FDOPA-PET is usually excellent and lies less than 10 mm. In this study even small parasympathetic head and neck PGLs with a minimal diameter of 6 mm have been clearly visualized, whereas the maximum spatial resolution of 123-I-MIBG scintigraphy in this study was 10 mm. Because these FDOPA-PET-negative tumors both showed a strong VMAT-1 and -2 expression, other factors in addition to VMATs might be responsible for the observed FDOPA-PET negativity. Before ^{18}F-FDOPA is translocated via VMATs to the storage vesicles, it enters the cells via specific amino acid transporters and is subsequently decarboxylated to dopamine by the enzyme L-amino acid decarboxylase, which is strongly expressed in neuroendocrine cells and shows high affinity to ^{18}F-FDOPA (8). A low or absent expression of this enzyme or the amino acid transporters regulating tracer uptake in PHEOs/PGLs could be an explanation for the observed FDOPA-PET negativity.

The characterization of a differentiated VMAT expression pattern of the PGLs investigated in this study allowed a clear separation of sympathetic from parasympathetic PGLs. All parasympathetic PGLs were VMAT-1 negative and did not express TH. The literature only suggests the use of TH to differentiate between chromaffin and nonchromaffin paragangliomas (32). The additional staining for VMAT-1 provides an easy way for a histological classification of paragangliomas. Interestingly, CgA immunostaining was very weak or absent in all parasympathetic PGLs. This correlated with a normal serum CgA in all of these patients, indicating that CgA is not an appropriate tumor marker in patients with parasympathetic PGLs. In accordance with other studies, immunohistochemical evaluation of the proliferation marker Ki-67 was not helpful to determine malignancy (32, 33).

In summary, these results suggest that for classical adrenal PHEOs FDOPA-PET and 123-I-MIBG scintigraphy show equal sensitivities. However, for the localization of extraadrenal PHEOs/PGLs and in patients with hereditary PHEO syndromes, FDOPA-PET is the functional imaging modality of choice. A predominant secretion of norepinephrine/normetanephrine can be used as clinical indicator that in these patients 123-I-MIBG scintigraphy most likely fails to detect PHEOs and PGLs and FDOPA-PET has to be used for functional imaging.

Acknowledgments

Address all correspondence and requests for reprints to: Christian Fottner, M.D., I. Medical Clinic, Department of Endocrinology and Metabolism, University of Mainz, Langenbeckstrasse 1, 55131 Mainz, Germany. E-mail: fottner@endokrinologie.klinik.uni-mainz.de.

Disclosure Summary: The authors declare no conflicts of interest.

References

1. **Lenders JW, Eisenhofer G, Mannelli M, Pacak K** 2005 Phaeochromocytoma. Lancet 366:665–675
2. **Havekes B, Pacak K** 2008 Pheochromocytoma. Nat Clin Pract Cardiovasc Med 5:E1
3. **Neumann HP, Eng C** 2009 The approach to the patient with paraganglioma J Clin Endocrinol Metab 94:2677–2683
4. **Karagiannis A, Mikhailidis DP, Athyros VG, Harsoulis F** 2007 Pheochromocytoma: an update on genetics and management. Endocr Relat Cancer 14:935–956
5. **Erlic Z, Neumann HP** 2009 Diagnosing patients with hereditary paraganglial tumours. Lancet Oncol 10:741
6. **Pacak K, Eisenhofer G, Ahlman H, Bornstein SR, Gimenez-Roqueplo AP, Grossman AB, Kimura N, Mannelli M, McNicol AM, Tischler AS; International Symposium on Pheochromocytoma** 2007 Pheochromocytoma: recommendations for clinical practice from the First International Symposium. October 2005. Nat Clin Pract Endocrinol Metab 3:92–102
7. **Havekes B, Lai EW, Corssmit EP, Romijn JA, Timmers HJ, Pacak K** 2008 Detection and treatment of pheochromocytomas and paragangliomas: current standing of MIBG scintigraphy and future role of PET imaging. Q J Nucl Med Mol Imaging 52:419–429
8. **Vaidyanathan G** 2008 Meta-iodobenzylguanidine and analogues: chemistry and biology. Q J Nucl Med Mol Imaging 52:351–368
9. **Uccella S, Cerutti R, Vigetti D, Furlan D, Oldrini R, Carnevali I, Pelosi G, La Rosa S, Passi A, Capella C** 2006 Histidine decarboxylase, DOPA decarboxylase, and vesicular monoamine transporter 2 expression in neuroendocrine tumors: immunohistochemical study and gene expression analysis. J Histochem Cytochem 54:863–875
10. **Wiseman GA, Pacak K, O'Dorisio MS, Neumann DR, Waxman AD, Mankoff DA, Heiba SI, Serafini AN, Tumeh SS, Khutoryansky N,**

Jacobson AF 2009 Usefulness of 123I-MIBG scintigraphy in the evaluation of patients with known or suspected primary or metastatic pheochromocytoma or paraganglioma: results from a prospective multicentre trial. J Nucl Med 50:1448–1454

11. **Timmers HJ, Eisenhofer G, Carrasquillo JA, Chen CC, Whatley M, Ling A, Adams KT, Pacak K** 2009 Use of 6-[18F]-fluorodopamine positron emission tomography (PET) as first-line investigation for the diagnosis and localization of non-metastatic and metastatic phaeochromocytoma (PHEO). Clin Endocrinol (Oxf) 71:11–17
12. **Pacak K, Eisenhofer G, Goldstein DS** 2004 Functional imaging of endocrine tumors: role of positron emission tomography. Endocr Rev 25:568–580
13. **Brink I, Hoegerle S, Klisch J, Bley TA** 2005 Imaging of pheochromocytoma and paraganglioma. Fam Cancer 4:61–68
14. **Ilias I, Sahdev A, Reznek RH, Grossman AB, Pacak K** 2007 The optimal imaging of adrenal tumours: a comparison of different methods. Endocr Relat Cancer 14:587–599
15. **Havekes B, King K, Lai EW, Romijn JA, Corssmit EP, Pacak K** 2010 New imaging approaches to phaeochromocytomas and paragangliomas. Clin Endocrinol (Oxf) 72:137–145
16. **Jager PL, Chirakal R, Marriott CJ, Brouwers AH, Koopmans KP, Gulenchyn KY** 2008 6-L-18F-fluorodihydroxyphenylalanine PET in neuroendocrine tumors: basic aspects and emerging clinical applications. J Nucl Med 49:573–586
17. **Hoegerle S, Nitzsche E, Altehoefer C, Ghanem N, Manz T, Brink I, Reincke M, Moser E, Neumann HP** 2002 Pheochromocytomas: detection with 18F DOPA whole body PET—initial results. Radiology 222:507–512
18. **Hoegerle S, Ghanem N, Altehoefer C, Schipper J, Brink I, Moser E, Neumann HP** 2003 18F-DOPA positron emission tomography for the detection of glomus tumours. Eur J Nucl Med Mol Imaging 30:689–694
19. **Ilias I, Chen CC, Carrasquillo JA, Whatley M, Ling A, Lazúrová I, Adams KT, Perera S, Pacak K** 2008 Comparison of 6-^{18}F-fluorodopamine PET with ^{123}I-metaiodobenzylguanidine and ^{111}in-pentetreotide scintigraphy in localization of nonmetastatic and metastatic pheochromocytoma. J Nucl Med 49:1613–1619
20. **Ilias I, Yu J, Carrasquillo JA, Chen CC, Eisenhofer G, Whatley M, McElroy B, Pacak K** 2003 Superiority of 6-[18F]-fluorodopamine positron emission tomography versus [131I]-metaiodobenzylguanidine scintigraphy in the localization of metastatic pheochromocytoma. J Clin Endocrinol Metab 88:4083–4087
21. **Taïeb D, Tessonnier L, Sebag F, Niccoli-Sire P, Morange I, Colavolpe C, De Micco C, Barlier A, Palazzo FF, Henry JF, Mundler O** 2008 The role of 18F-FDOPA and 18F-FDG-PET in the management of malignant and multifocal phaeochromocytomas. Clin Endocrinol (Oxf) 69:580–586
22. **Kaji P, Carrasquillo JA, Linehan WM, Chen CC, Eisenhofer G, Pinto PA, Lai EW, Pacak K** 2007 The role of 6-[18F]fluorodopamine positron emission tomography in the localization of adrenal pheochromocytoma associated with von Hippel-Lindau syndrome. Eur J Endocrinol 156:483–487
23. **Fiebrich HB, Brouwers AH, Kerstens MN, Pijl ME, Kema IP, de Jong JR, Jager PL, Elsinga PH, Dierckx RA, van der Wal JE, Sluiter WJ, de Vries EG, Links TP** 2009 18F-DOPA PET is superior to conventional imaging with 123I-metaiodobenzylguanidine scintigraphy, CT, and MRI in localizing tumors causing catecholamine excess. J Clin Endocrinol Metab 94:3922–3930
24. **Anlauf M, Eissele R, Schäfer MK, Eiden LE, Arnold R, Pauser U, Klöppel G, Weihe E** 2003 Expression of the vesicular monoamine transporter (VMAT1 and VMAT2) in the endocrine pancreas and pancreatic endocrine tumors. J Histochem Cytochem 51:1027–1040
25. **Koopmans KP, Neels OC, Kema IP, Elsinga PH, Sluiter WJ, Vanghillewe K, Brouwers AH, Jager PL, de Vries EG** 2008 Improved staging of patients with carcinoid and islet cell tumors with 18F-dihydroxy-phenyl-alanine and 11C-5-hydroxy-tryptophan positron emission tomography. J Clin Oncol 26:1489–1495
26. **Schuldiner S, Shirvan A, Linial M** 1995 Vesicular neurotransmitter transporters: from bacteria to humans. Physiol Rev 75:369–392
27. **Weihe E, Eiden LE** 2000 Chemical neuroanatomy of the vesicular amine transporters. FASEB J 14:2435–2449
28. **Peter D, Jimenez J, Liu Y, Kim J, Edwards RH** 1994 The chromaffin granule and synaptic vesicle amine transporters differ in substrate recognition and sensitivity to inhibitors. J Biol Chem 11; 269:7231–7237
29. **Erickson JD, Schafer MK, Bonner TI, Eiden LE, Weihe E** 1996 Distinct pharmacological properties and distribution in neurons and endocrine cells of two isoforms of the human vesicular monoamine transporter. Proc Natl Acad Sci USA 93:5166–5171
30. **Peter D, Liu Y, Sternini C, de Giorgio R, Brecha N, Edwards RH** 1995 Differential expression of two vesicular monoamine transporters. J Neurosci 15:6179–6188
31. **Huynh TT, Pacak K, Brouwers FM, Abu-Asab MS, Worrell RA, Walther MM, Elkahloun AG, Goldstein DS, Cleary S, Eisenhofer G** 2005 Different expression of catecholamine transporters in phaeochromocytomas from patients with von Hippel-Lindau syndrome and multiple endocrine neoplasia type 2. Eur J Endocrinol 153:551–563
32. **Tischler AS** 2008 Pheochromocytoma and extra-adrenal paraganglioma: updates. Arch Pathol Lab Med 132:1272–1284
33. **Tischler AS, Kimura N, Mcnicol AM** 2006 Pathology of pheochromocytoma and extra-adrenal paraganglioma. Ann NY Acad Sci 1073:557–570